

December 21, 1988

TITLE: Indirect Coal Liquefaction: Direct Catalytic Conversion of Methane and Light Hydrocarbon Gases

AUTHORS: Robert B. Wilson Jr., Yee-Wai Chan, and Barry Posin

ORGANIZATION: SRI International
333 Ravenswood Ave.
Menlo Park, CA 94025
Tel: 415-859-5954

CONTRACT NO: DE-AC22-86PC90011

PERIOD OF PERFORMANCE: 24 Sept. 1986 - 24 Sept. 1989

INTRODUCTION

The goal of this program is to explore novel ways to directly convert methane and light hydrocarbons to useful chemicals that can themselves be converted to either transportation fuels or to chemical feedstocks. We have taken two distinct approaches: First, direct conversion by dehydrocoupling reactions using supported organometallic complexes. Second, partial oxidation using supported homogeneous oxidation catalysts such as porphyrins and phthalocyanines. This paper will review our results in both areas with emphasis on the oxidation since our submissions in previous years have concentrated on the dehydrocoupling. In addition, we will introduce our recent work using in-situ diffuse reflectance FTIR at high temperature to study these and other reactions at realistic pressure and flow conditions.

DEHYDROCOUPLING OF METHANE BY
SUPPORTED ORGANOMETALLIC COMPLEXES

INTRODUCTION

Two possibilities exist for the dehydrocoupling of methane to higher hydrocarbons: The first is oxidative coupling which is currently an area of intense research, including several of the other DOE contractors whose papers also appear in this volume. However, an alternative is the non-oxidative coupling where the co-product is hydrogen. The thermodynamics of the two processes are compared in Table 1.¹ The oxidative coupling process is exothermic but the process is difficult to control because continued oxidation (eventually to complete combustion) is even more exothermic. The dehydrocoupling route is endothermic and the degree of endothermicity increases with extent of dehydrogenation. Thus, while it is necessary to input energy to accomplish the reaction it is, in principal, a more easily controlled process. The coking of the catalyst is not shown in Table 1, but is a process that accompanies these dehydrogenation reaction. It is control of this coking that is the key difficulty in making use of dehydrocoupling reactions for methane. Mitchell and Waghorne reported the major product of methane dehydrogenation using an alumina supported CaCrPt catalyst under anaerobic condition was benzene.² Jones et al. also observed small amounts of benzene produced from the methane reforming over silica support GeO₂.³

Table I
Thermodynamics for Dehydrocoupling Reactions of Methane¹

	<u>$\Delta G_{427^\circ\text{C}}$ (Kcal/mol)</u>
$2 \text{ CH}_4 \longrightarrow \text{C}_2\text{H}_6 + \text{H}_2$	+10
$2 \text{ CH}_4 \longrightarrow \text{C}_2\text{H}_4 + 2 \text{ H}_2$	+20
$2 \text{ CH}_4 \longrightarrow \text{C}_2\text{H}_2 + 3 \text{ H}_2$	+35
$2 \text{ CH}_4 + \frac{1}{2} \text{ O}_2 \longrightarrow \text{C}_2\text{H}_6 + \text{H}_2\text{O}$	-25
$2 \text{ CH}_4 + \text{ O}_2 \longrightarrow \text{C}_2\text{H}_4 + 2 \text{ H}_2\text{O}$	-45
$2 \text{ CH}_4 + \frac{3}{2} \text{ O}_2 \longrightarrow \text{C}_2\text{H}_2 + 3 \text{ H}_2\text{O}$	-95

An indication that the dehydrocoupling of methane can be achieved comes from chemisorption studies of methane on metals. Table 2 contains a collection of the temperature of dissociative chemisorption of methane on a number of metals.⁴ These values are determined by measuring the appearance of hydrogen in the gas mixture above these metals in the presence of methane.

Table 2
Temperature of Dissociative Chemisorption⁴

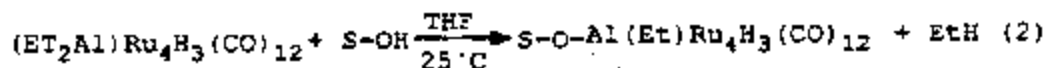
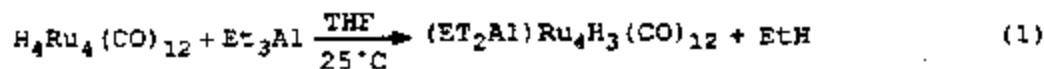
<u>METAL</u>	<u>T_{H2}(°C)</u>
Re	20
Rh	50
Mo	80
Ni	100
Pd	125
Ta	225
Ti	320

Research on the technique of surface confinement to produce novel catalysts for a wide variety of processes is continuing in many laboratories.⁵⁻⁸ We have been working on the development of novel surface confined catalysts to dehydrocouple methane. The catalysts are prepared by reacting organometallic complexes of transition metals with inorganic oxide supports to produce surface-confined metal complexes.⁹ The metal complexes decompose to obtain very stable, highly dispersed catalysts. The increased activity of highly dispersed catalysts is desirable for activating the relatively inert methane, and additionally highly dispersed catalysts are resistant to coking. The use of zeolitic supports will provide further stabilization of the highly dispersed catalysts which are confined inside the zeolite pores. The variables we are studying include cluster size, supporting materials, and reaction conditions.

Synthesis of catalysts- The synthesis of these catalysts involves three steps. The first step is to synthesize the ruthenium cluster precursors. The second step is a novel approach developed in our laboratory involving the reaction of the organometallic clusters with alkyl aluminum. The final step is to anchor these catalysts on supports by a chemical reaction

between the hydroxy group of the support and the alkyl groups of the organometallic cluster to give a covalent chemical bond.

The organometallic complexes include: a mono-ruthenium complex, $\text{Ru}(\text{allyl})_2(\text{CO})_2$; a tetrameric ruthenium cluster, $\text{H}_4\text{Ru}_4(\text{CO})_{12}$; a hexameric ruthenium cluster, $\text{H}_2\text{Ru}_6(\text{CO})_{18}$; and a mixed metal cluster, $\text{H}_2\text{FeRu}_3(\text{CO})_{13}$. All of these complexes are prepared according to literature procedures.^{10,11} The hydrido clusters reacted with triethyl aluminum at room temperature (eq. 1). The reaction stoichiometries are determined by measuring the quantity of ethane produced.⁹ These alkyl aluminum carbonyl ruthenium clusters react with acidic supports: β -alumina, 5A molecular sieves, and LZ-Y 52 zeolite. The reaction stoichiometries are again determined by measuring the quantity of ethane produced (eq. 2).



The monomeric ruthenium complex reacts directly with the acidic support to release one equivalent of propylene. The tetraruthenium and the mixed iron-ruthenium clusters have also been supported on magnesium oxide by the reaction of the acidic hydride and the basic groups on the MgO surface. All supporting materials are in powder form except for the 5A molecular sieves which was 60-80 mesh.

RESULTS AND DISCUSSION

The ruthenium catalysts were tested at 750°C under 150 psig pressure. Three different sizes of ruthenium clusters: monomer (Ru), tetramer (Ru_4), and hexamer (Ru_6) were supported on three different supports: β -alumina, 5A molecular sieve, and Y-zeolite. The results are summarized in Table 3. We used a commercial ruthenium catalyst which is supported on alumina (obtained from Engelhard) for comparison. The metal loadings were based on elemental analyses (Galbraith Laboratory). The flow-rate of input gases (20% methane in helium) were varied due to the detection limit of our GC. Effect of flow-rate will be discussed later.

Effects of cluster size - The commercial ruthenium catalyst gives a very high conversion of methane (71.2%) but no hydrocarbon product. Methane conversion on the mono-ruthenium catalysts are considerably lower than the ruthenium clusters (Ru_4 and Ru_6). In general, methane conversions depend on the type of support and decrease in the order alumina, 5A molecular sieve, and zeolite. These results suggested that the methane conversion is related to the amount of surface bonded metal. On alumina, the metals are located on the surface while on 5A molecular sieves and on zeolite, increasing amounts of metal are located inside the zeolite pore. The Ru_4 catalysts demonstrated the greatest dependance on the support, the conversion decreased from 10.1 to 4.9 and to 1.7% on alumina, 5A molecular sieve, and Y-zeolite, respectively.

Our intention in using different supports is to confine the ruthenium cluster at different location on or within the support. Hence, the Ru_4 and Ru_6 clusters are dispersed on the alumina surface but are confined inside the pores of the zeolite supports. The pore size of the 5A molecular sieve is too small for the Ru_6 cluster but should be large enough for the Ru_4 cluster. Since the Y-zeolite has the largest pore ($\sim 17\text{\AA}$), most of the Ru_4 or Ru_6 clusters are located inside the zeolite pore.

Product selectivity

All the ruthenium catalysts produced C_2 hydrocarbons which included ethane and ethylene. The selectivity of C_2 hydrocarbon observed with Ru_4 cluster catalysts increased as the percent conversion of methane decreased. These results also suggest the advantage of having the metal cluster confined inside the zeolite cage. The Ru_6AL has the highest total hydrocarbon yield which is probably due to the higher metal loading. The total hydrocarbon yield for Ru_6MS and Ru_6ZL are about the same, but the Ru_6ZL has a higher selectivity for C_2 product. Confining the metal cluster inside the zeolite cage may also limited the propagation of methane polymerization. The ruthenium monomers gave relatively low hydrocarbon yields indicating that polymerization of methane required more than one metal atom.

Table 3

ACTIVITY OF RUTHENIUM CATALYSTS FOR METHANE DEHYDROGENATION^a

Catalyst ^b	Ru (wt%)	Flow rate (mL/min)	Methane Conver (%)	% Selectivity ^c to		
				H ₂	C ₂	C ₆ ^d
Ru-com	0.50	50	71.2	151.0	-- ^d	--
RuAL	0.35	10	3.0	139.9	2.8	--
RuMS	0.31	10	2.3	147.5	1.2	--
RuZL	0.37	10	1.7	177.5	2.6	--
Ru ₄ AL	0.61	100	10.1	78.6	1.62	--
Ru ₄ MS	0.49	100	4.9	146.6	3.52	--
Ru ₄ ZL	0.61	50	1.7	25.3	6.9	28.9
Ru ₆ AL	1.26	50	6.1	113.4	6.9	41.4
Ru ₆ MS	0.19	50	5.6	192.8	1.0	14.8
Ru ₆ ZL	0.20	50	3.6	161.9	3.6	10.0

^aReaction condition: temperature=750°C, pressure=150 psig

^bAbbreviation: Ru-com=commercial ruthenium catalyst from Engelhard; Ru₄=(C₂H₅)₂AlRu₄H₃(CO)₁₂; Ru₆=(C₂H₅)₂AlRu₆H(CO)₁₈; Ru=Ru(Allyl)(CO)₂; AL=B-alumina; MS=5A molecular sieve; ZL=LZ-Y zeolite.

^cSelectivities were calculated on converted methane. Selectivity to hydrocarbons are based on carbon number.

^dNot detected.

Coking

The results listed in Table 3 show that more than one equivalent of hydrogen was produced per methane input, which suggests that some of the methane turned to coke. The elemental analyses listed in Table 4 showed that the Ru₄AL, Ru₄MS, Ru₆AL and Ru₆MS contained more carbon after reacted with methane. In contrast, the carbon contents in Ru₄ZL decreased after reactions. This phenomena indicated that those catalysts having metal dispersed on the support surface promote coke formation while the metals being confined inside the zeolite cages does not. For the Ru₄MS, the carbon content only increased slightly to 4.38% as compare to more than 20% for the Ru₄ZL suggest that a portion of the metal clusters are located inside the cages of the support. The decrease of carbon content on Ru₄ZL was due to the decomposition of the ruthenium complexes, i.e. release of carbon monoxide.

Table 4
ELEMENTAL ANALYSES OF RUTHENIUM CATALYSIS FOR METHANE
REFORMING^a

Catalyst	Before reaction			After reaction		
	%C	%H	%Ru	%C	%H	%Ru
Ru ₄ AL	5.09	1.04	0.61	26.50	0.40	0.57
Ru ₄ MS	1.46	1.13	0.49	4.38	0.46	0.64
Ru ₄ ZL	5.25	1.53	0.61	0.58	0.22	1.26
Ru ₆ AL	9.77	1.84	1.26	23.24	0.67	0.55
Ru ₆ MS	0.95	1.68	0.19	22.29	0.19	0.32

^aReaction with methane at 750°C for 15 h.

Effect of reaction conditions

The effect of reaction temperature is similar for every catalyst. Higher methane conversion and product yield are obtained at higher temperature. These results are expected because polymerization of methane is thermodynamically unfavored process.¹² Increasing the reaction pressure has a similar effect on the methane conversion. However, the product selectivities for hydrogen and C₂ hydrocarbons decrease but increases for C₆₊ hydrocarbons (Table 5). Highest selectivity is observed at 150 psig. As expected, increasing the space velocity lower the methane conversion but increase the selectivity of hydrocarbon products.

Table 5
EFFECT OF REACTION PRESURE AND SPACE VELOCITY TO
THE ACTIVITY OF Ru₆ZL^a AT 750°C

Pressure (psig)	Flow rate mL/min	%CH ₄ conversion	%Selectivity ^b of		
			H ₂	C ₂	C ₆₊
50	50	3.18	164.16	6.04	6.6
150	50	5.19	91.33	4.48	10.70
250	50	8.64	82.41	2.46	7.38
250	100	2.62	177.10	9.24	20.64

^aRu₆ZL = zeolite supported Ru₆ cluster, C₂H₅AlRu₆H(CO)₁₈.

^bSelectivity was based on carbon number of hydrocarbon and the amount of methane reacted.

Basic support and mixed metal cluster

Methane conversion of the magnesia supported ruthenium monomer and the FeRu₃ cluster are much higher than the zeolite supported analogs (Table 6). However, the product selectivities to hydrocarbons are lower.

For the mixed iron-ruthenium catalysts, magnesia support also increased the methane conversion. At 600°C, the methane conversion was 8.87% for FeRu₃MgO and was 3.07% for FeRu₃ZL. At 750°C, methane conversion increased to 41.5% and 23.05% for FeRu₃MgO and FeRu₃ZL, respectively. These catalysts behave similarly to the ruthenium monomers that the hydrocarbon yields were lower on the magnesia supported catalyst.

Table 6
CATALYTIC REACTIVITY OF ZEOLITE AND MAGNESIA
SUPPORTED CATALYSTS FOR METHANE DEHYDROGENATION^a

Catalysts	Temp (°C)	Methane Conversion (%)	Selectivity ^b	
			C ₂ (%)	C ₆₊
RuMgO	600	21.044	0.1	0.5
Ru ₄ MgO	750	4.04	6.9	49.2
FeRu ₃ ZL	600	3.07	1.9	18.5
FeRu ₃ MgO	600	8.87	0.1	--

^aReaction conditions: pressure=150psig, flow rate=20 mL/min, weight of catalyst=2 g, reactor O.D.=3/8in (S.S.).

^bSelectivity to hydrocarbon is based on carbon number.

^cNot detected.

Increased temperature has a similar effect on the methane conversion over FeRu₃ZL, but the methane conversion was lower than the MgO supported catalysts. At 750°C, the methane conversion was 23.05%. Hydrocarbon yields increased as the reaction temperature increased from 500° to 600°C and then declined at higher temperature. The maximum yield of C₂ was 0.06% of the input methane and was 0.57% for C₆₊. Since the Ru₄ZL was essentially nonactive at 600°C, this low temperature reactivity of FeRu₃ZL is obviously due to an effect of the mixed metal. Introduction of the iron to the metal cluster is advantageous to methane dehydrogenation activity. Figure 1 shows the effect of

increasing temperature on methane conversion and on hydrocarbon yield. Highest hydrocarbon yield was obtained at 600°C. However, the hydrogen selectivity was 170% at this temperature which suggests coke formation.

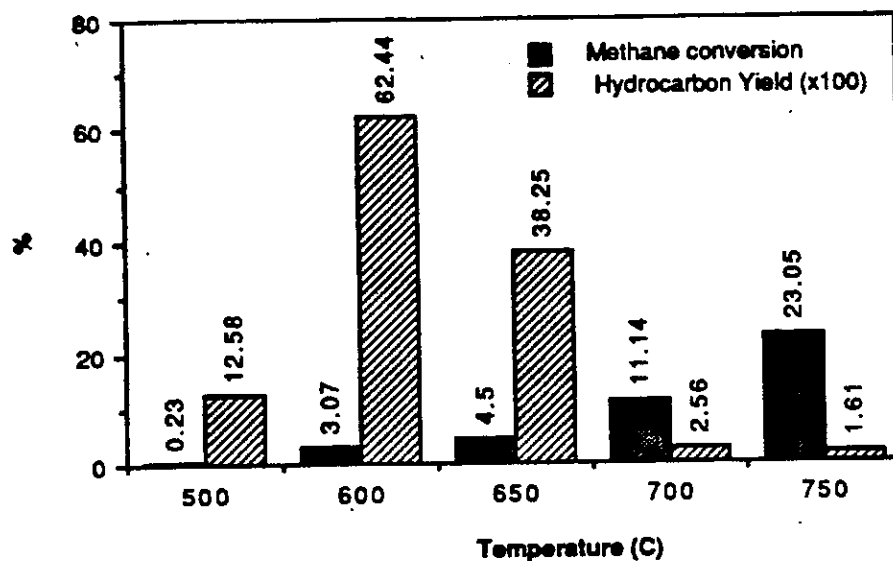


Figure 1. Activity of FeRu₃ZL for methane dehydrocoupling at various temperatures.

PARTIAL OXIDATION OF METHANE USING SUPPORTED PORPHYRIN AND PHTHALOCYANINE COMPLEXES

INTRODUCTION

Conversion of methane to useful chemicals by partial oxidation and oxidative dehydrogenation has received much attention of many researchers.¹ Ever since Balair and Wheeler first demonstrated that methane can be oxidized in the presence of a catalyst, there have been a number of reports dealing with the partial oxidation of methane using a variety of techniques and catalysts.^{8,9,13,14} Our approach to selective partial oxidation of methane is to synthesize encapsulated porphyrin and phthalocyanine complexes. These complexes are homogeneous selective oxidation catalysts that mimic the remarkable enzyme Cytochrome P-450. Porphyrins and phthalocyanines are potent oxidants that also allow careful control of the active form of oxygen, thereby leading to control of activity and selectivity. The use of zeolitic supports will enhance the stability and reactivity of the catalysts, and will discourage the secondary reactions that always pose problems in the oxidation of methane because the primary products are more easily oxidized than methane.

RESULTS AND DISCUSSION

Phthalocyanine complexes are synthesized within the zeolite pore by first exchanging the metal ion into the pore, followed by template condensation. We use Na-Y zeolite because it has large pores that allow the phthalocyanine complexes to fit in and contains exchangeable ions. Some of the phthalocyanine absorbed on the zeolite surface and are removed by extraction with pyridine and acetone. Excess metal ions are then back exchanged with sodium ions. Surface reflectance UV-Vis and FT-IR of the non-extracted catalysts confirm the presence of phthalocyanine.

The zeolite encapsulated metalloporphyrins are synthesized by a second method; the metal free ligand is first synthesized inside the zeolite cage by refluxing benzaldehyde, pyrrol, and the Na-Y zeolite (without metal exchange) in acetic acid. The surface attached porphyrin is extracted with methanol. The washing contains tetraphenylporphyrin as indicated by its UV-Vis spectrum.

The desired metal ion is inserted into the porphyrin by boiling the metal salt and the zeolite containing the porphyrin in dimethylsulfoxide solution. The product is washed with

water and then Soxhlet extracted with methanol to remove surface-bound TPP complex. Uncomplexed metal ions are removed by reverse ion-exchange with sodium chloride. However, the excess iron ions are not exchangeable by sodium ions and we have not attempted to remove the excess iron by other methods. The FePCZL and the FeTPPZL thus contained excess iron ions. The metal loading (by weight) and the percent of super cages occupied by the metal complexes (calculated based on the results from elemental analyses) are listed in Table 7.

Table 7
ELEMENTAL ANALYSIS OF METHANE OXIDATION CATALYSTS

Catalyst ^a	Wt. % metal Loading	% Complex Loading
CoPCZL	1.53	60
FePCZL	4.15 ^b	50
RuPCZL	0.97	20
MnPCZL	1.62	68
CoTPPZL	0.15	5
FeTPPZL	4.04 ^b	8
RuTPPZL	0.13	2.5
MnTPPZL	0.12	4.3

^apc = phthalocyanine, TPP = Tetraphenylporphyrin, ZL = zeolite
^bThe iron complexes contained excess iron ions which can not be exchanged by sodium ions.

We tested these zeolite catalysts for methane oxidation at 375 °C under 50 psig pressure. Methane to oxygen feed ratio was 4 and the GHSV was about 2600 h⁻¹. Catalysts were activated under hydrogen flow at 200 °C for 2 h before the introduction of the methane/oxygen mixture.

The methane reaction results were averaged from data taken during the 15 to 20 h of the runs and are summarized in table 8. Three catalysts including RuPcZL, CoTPPZL, and MnTPPZL showed activity toward the formation of methanol. As shown in table 8, the RuPcZL gave the highest selectivity of methanol. The methane conversions were generally below 10%. Carbon dioxide and water were always the major products.

Three control experiments were run using the blank zeolite, ruthenium exchanged zeolite (with triruthenium dodecacarbonyl), and Ruthenium tetracarboxyphthalocyanine. The blank zeolite gave essentially no methane oxidation activity. Less than 0.5% of methane

was oxidized to carbon dioxide. The ruthenium zeolite produced hydrogen, carbon dioxide and water with approximate 16% methane conversion. The RuTPPZL and FePcZL also gave hydrogen which suggest that these two catalysts behave like the simple metal exchanged zeolite. Because the excess metal ion in this two catalysts were not removed by the reverse ion exchange process. The productions of hydrogen were due to the catalytic ability of the zeolite adsorbed metal particles. We have observed the similar result from the ruthenium cluster bonded zeolite. At 400 °C and a CH₄/O₂ ratio of 10, Ru₄ZL gave 30.7% of hydrogen and 61.6% of carbon dioxide with 18.9% methane conversion.

In the absence of zeolite support, RuTCPC does not convert methane to desired product. Only 1.7% of methane was consumed and the products were carbon dioxide and water. A slight excess of water was produced due to the decomposition of the peripheral substituent (-COOH). The choice of TCPC was simply because of its availability in our laboratory.

Table 8
ACTIVITY OF METHANE OXIDATION CATALYSTS

Catalyst	% Conver of CH ₄	% Selectivity			
		H ₂	CO ₂	H ₂ O	CH ₃ OH
Zeolite	0.5	---	100	---	---
RuZL	15.9	45	100	100	---
RuTCPC	1.7	---	100	206	---
CoPcZL	6.3	---	100	100	---
FePcZL	18.2	1.2	100	42	---
RuPcZL	4.8	---	87	1	11.3
MnPcZL	9.6	---	80	65	---
CoTPPZL	1.9	---	94	120	5.8
FeTPPZL	1.9	---	100	73	---
RuTPPZL	8.4	50	99	146	---
MnTPPZL	1.8	---	95	126	3.5

Reaction conditions: Temperature=375 °C, Pressure=50psig,
CH₄/O₂=4, GHSV=2600 h⁻¹.

Some of the catalysts were also tested at higher temperature under the same condition. The results were averaged from 4 h runs and were summarized in Table 9. Methane conversions were generally increased. Again, only RuPcZL and CoTPPZL showed some

reactivity on methanol formation, but the yields were significantly decreased. These results indicated that the metal complexes decomposed at high temperature. Table 10 listed the elemental analysis results of the catalysts after reaction with methane and oxygen at 450 °C. The carbon contents decreased to less than 0.2% except for the RuTPFZL which remained approximately the same. RuTPP may be more stable than the other complexes. In the case of CoPCZL, we observed a mixture of hydrocarbon released during the first hour of reaction at 375 °C.

Table 9
Activity of Methane Oxidation catalyst

Catalyst	Temp (°C)	% conver		% Selectivity			
		CH ₄	O ₂	H ₂	CO ₂	H ₂ O	CH ₃ OH
RuZL	375	15.9	99.0	45.0	100.0	100.0	---
	500	20.8	99.0	110.0	89.3	---	---
FePcZL	375	18.2	53.9	1.2	100.0	42.5	0.0
	500	22.7	87.2	15.9	100.0	45.0	---
RuPcZl	375	4.8	14.5	---	87.5	0.5	11.3
	450	9.0	99.6	---	96.7	0.5	3.3
CoTPPZL	375	1.9	15.1	---	94.3	119.7	5.8
	450	3.3	56.1	---	98.0	126.2	2.0
FeTPPZL	375	1.9	15.1	---	100.0	---	---
	450	6.1	32.8	---	100.0	65.1	---

Reaction conditions: Pressure=50psig, CH₄/O₂=4, GHSV=2600 h⁻¹.

Table 10
 ELEMENTAL ANALYSIS OF METHANE OXIDATION CATALYSTS
 AFTER REACTION WITH METHANE AND OXYGEN AT 450 °C

Catalyst ^a	% C	% H ₂	% N ₂	% Metal
FePcZL-b	8.06	1.51	1.98	4.15
-c	0.10	0.46	<0.05	3.46
RuPcZL-b	2.30	1.68	0.42	0.97
-c	0.13	1.00	0.10	0.89
CoTPPZL-b	2.36	1.01	0.41	0.15
-c	0.19	0.47	0.26	0.20
FeTPPZL-b	2.36	1.04	0.48	4.04
-c	0.20	0.69	<0.10	4.03
RuTPPZL-b	2.46	1.13	0.52	0.13
-c	2.13	0.99	0.32	0.14

^aPc=phthalocyanine, TPP=Tetraphenylporphyrin, ZL=zeolite

^bBefore reaction

^cAfter reaction of methane and oxygen at 450 °C

Table 11
 METAL LOADING AND COMPLEX LOADING OF THE
 MAGNESIUM OXIDE SUPPORTED CATALYSTS

Catalyst	Metal loading (Wt%) ^a	Complex loading (mol/100g) ^b
FeTSPCMgO	0.24	0.052
RuTSPCMgO	0.45	0.047
PdTSPCMgO	0.18	0.026
CuTSPCMgO	0.37	0.054
MoTSPCMgO	10.21	0.057

^aBased on elemental analysis

^bMole of complex were calculated based on the carbon weight from the elemental analyses.

We tested the MnTSPCMgO and MoTSPCMgO for methane oxidation under the conditions used for testing the catalysts reported last month. Both catalysts gave only

carbon dioxide and water. No hydrocarbon or methanol was detected. Methane conversions were less than 1% at temperature ranging from 375°C to 450°C (Table 12). We also ran a control reaction using blank magnesium oxide. The blank support also oxidized methane to carbon dioxide and water under these conditions. The methane consumption was slightly higher for the blank than observed for the MnTSPCMgO and the MoTSPCMgO.

Table 12
ACTIVITY OF MgO SUPPORTED METHANE OXIDATION CATALYSTS^a

Catalysts	Temp. (°C)	%Conversion of methane	%Selectivity ^b	
			CO ₂	C ₂ H ₆
PdTSPCMgO	375	1.4	60.2	3.5
	400	2.6	86.9	3.9
	450	5.7	98.2	0.6
FeTSPCMgO	375	0.8	42.1	0.0
	400	0.6	50.7	0.0
	450	1.5	84.6	0.0
RuTSPCMgO	375	1.3	62.1	0.0
	400	2.0	75.4	0.0
	450	2.6	90.7	0.0
CoTSPCMgO	375	0.6	40.6	0.0
	400	0.8	46.5	0.0
CuTSPCMgO	375	0.7	40.0	0.0
MnTSPCMgO	375	0.6	13.6	0.0
	400	0.5	34.5	0.0
MoTSPCMgO	375	0.8	27.5	0.0
	400	0.7	40.6	0.0
	450	0.9	55.7	0.0
MgO	375	0.8	42.7	0.0
	400	1.6	14.7	0.0
	450	1.9	47.3	0.0

^aCondition: Pressure = 1 atm, CH₄/O₂ = 10, GHSV = 5000 h⁻¹.

^bSelectivity of carbon products was calculated based on carbon number. Carbon dioxide and ethane were the only carbon product detected from these reactions.

The data in Table 12 indicates that MgO supported phthalocyanine complexes do not catalyze the partial oxidation of methane to methanol. However, it is interesting that the PdTSPCMgO produced ethane from the reaction. We suspect that the methanol produced underwent further oxidation to CO₂ and hydrocarbons.

We modified our reaction system to allow methanol to be fed into the reactor. Helium was used to dilute methanol at a ratio of approximately 10:1 of He:MeOH. We tested an empty reactor, Na-Y zeolite, and MgO for activity. In a separate run over MgO, oxygen was added to test if it increases methanol decomposition. The results are listed in Table 4. Methanol started to decompose at 300°C in an empty reactor and the only detectable product was methane. At 375°, 1.2% of the input methanol was converted to CO₂ and hydrocarbons. The conversion was higher in the presence of zeolite or magnesia (8.5 and 12.2%, respectively). Zeolite gave a very high selectivity of hydrocarbons. Approximately 85% of the methanol was converted to hydrocarbons. The methanol consumption on MgO was higher but the selectivity to hydrocarbons was lower than that on zeolite. In the presence of oxygen, almost 78% of the methanol was decomposed on MgO and 96.4% of that was oxidized to carbon dioxide.

IN-SITU DIFFUSE REFLECTANCE FTIR STUDIES OF METHANE CONVERSION CATALYSIS

We have begun to use In-Situ FTIR as a method to study the mechanisms of heterogeneous catalysis. We are using the sample holder shown in Figure 2 for these studies. The sample holder fits into a pressure chamber which is equipped with IR windows that are capable of withstanding several hundred psi and are water cooled. The reactive gas is inlet into this pressure chamber and flows out through the sample as shown. The sample is heated and the temperature controlled using a thermocouple imbedded in the powder sample. It is required that the sample not be powdered and that it not be strongly absorbing in the IR. This diffuse reflectance FTIR (DRIFTS) is very similar to the one recently reported by Vannice.¹⁵ We have been able to collect data using this system up to 600 °C. We are unable to collect good spectra at 700°C. We have noticed that at this temperature the heating block is glowing red rather than its normal black color, and this change may be connected with our ability to collect good spectral information at this temperature.

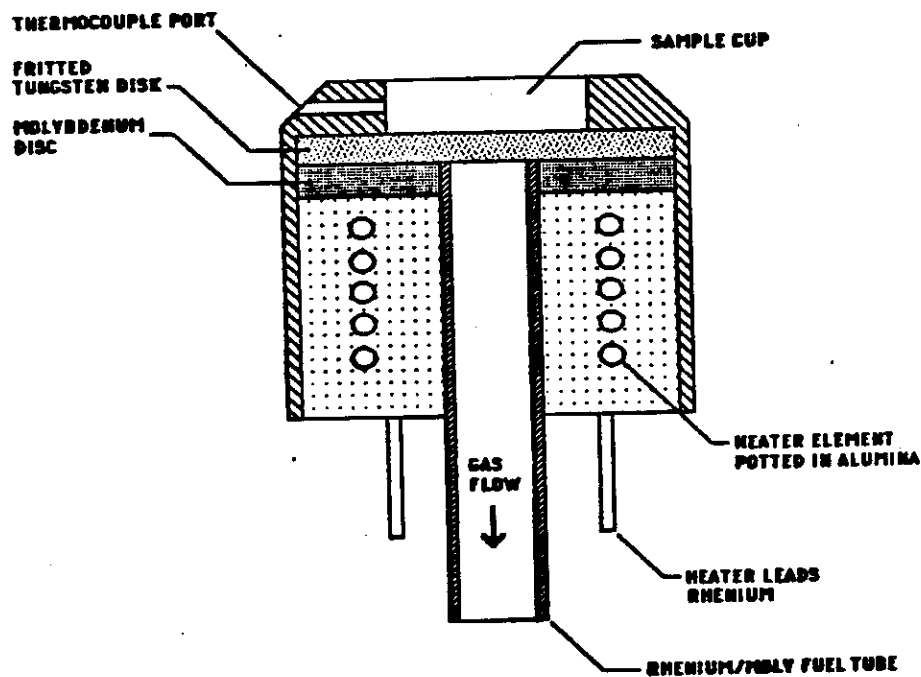
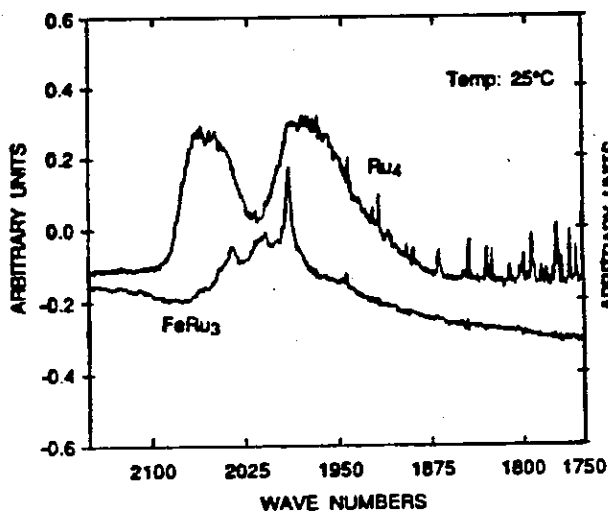


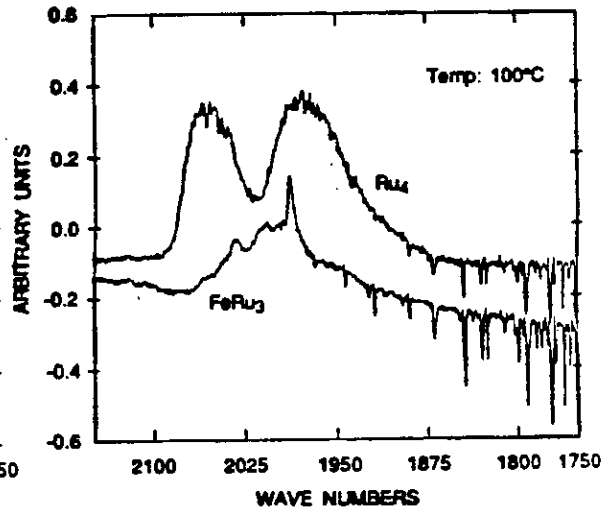
Figure 2: Sample Holder for In-Situ Diffuse Reflectance FTIR Studies of Supported Catalysts For Methane Conversion.

Figure 3 demonstrates the kind of data that can be collected using this FTIR technique. In Figure 3 we have compared the thermal behavior of two of the clusters (FeRu_3 and Ru_4) supported on MgO under N_2 . The carbonyl stretching region of the spectra is shown starting in the upper left at 25 °C. The two spectra are different as would be expected for the different clusters. However, more dramatic is the difference in thermal behavior. The FeRu_3 cluster has drastically changed by 200 °C and has completely disappeared by 300 °C. The Ru_4 cluster is considerably more robust maintaining most of its features to 300 °C.

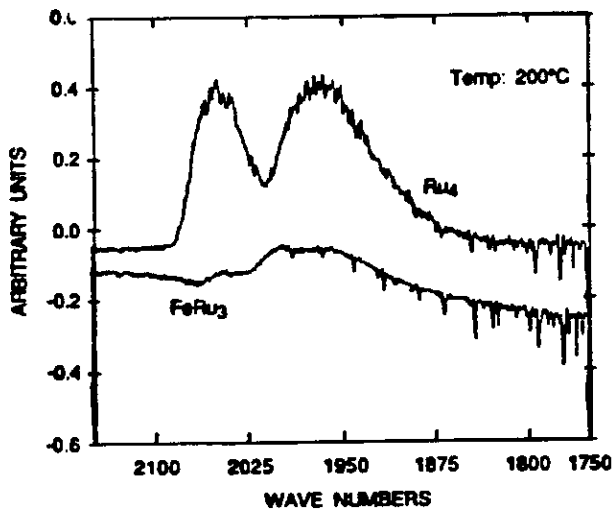
We then started with fresh samples and studied their IR behavior in flowing 5% methane in argon to simulate the conditions that we use in our dehydrocoupling experiments. The results were quite dramatic and are shown in Figure 4. The spectra are shown starting at 25 °C on the bottom left. Here clearly the FeRu_3 cluster begins to interact with the methane even at room temperature, while the Ru_4 has the identical spectra to that observed under nitrogen. Notice the increased intensity of the absorption, here over 6 units while under nitrogen the spectra of FeRu_3 had an intensity of less than 0.2 units, and also the loss of features (compare to upper left spectra of Figure 3). However, by 400 °C the two spectra have become identical (bottom right of Figure 4), a broad feature less absorption. This contrast to the spectra under nitrogen where by 400 °C both clusters and completely lost their absorption. We are currently attempting to interpret these results and to study the C-H stretching region of the spectra to learn more about hydrocarbon fragments on the catalysts.



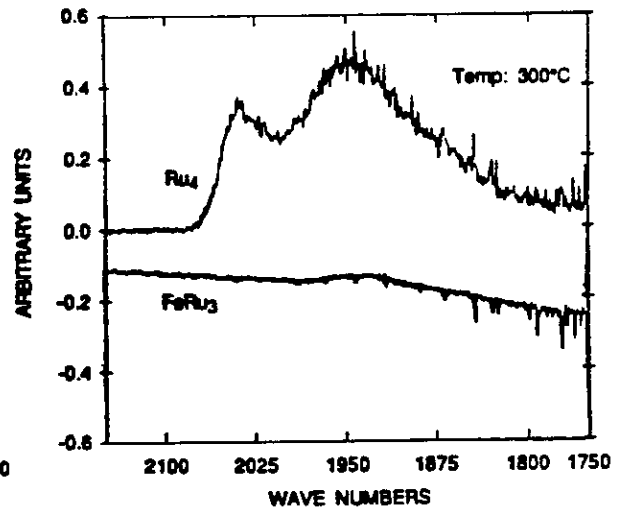
RA-2578-25



RA-2578-35

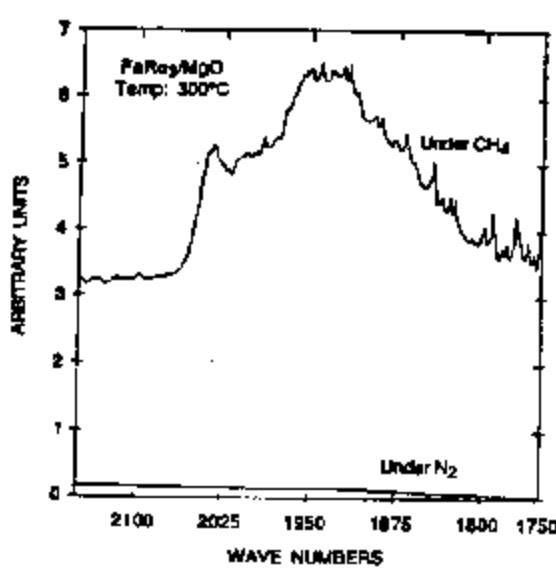


RA-2578-57

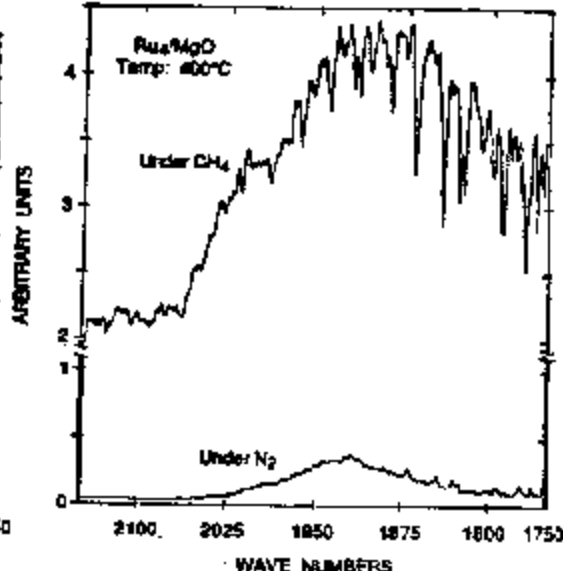


RA-2578-85

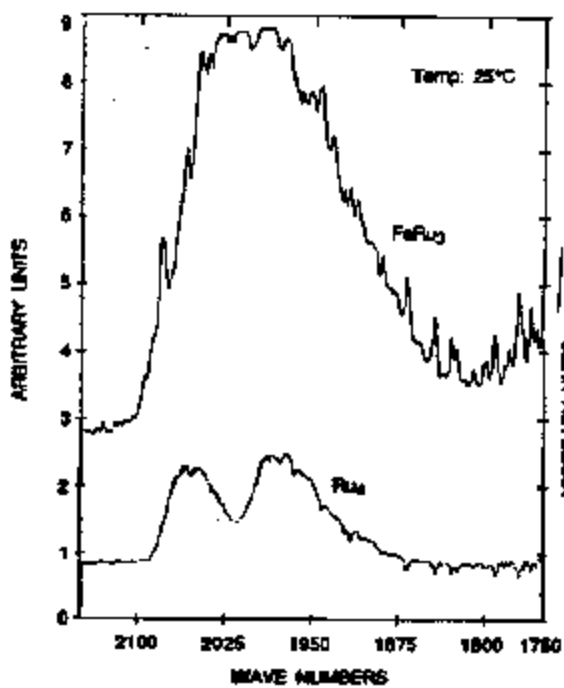
Figure 3: Comparison of Ru₄ and FeRu₃ clusters on MgO under N₂



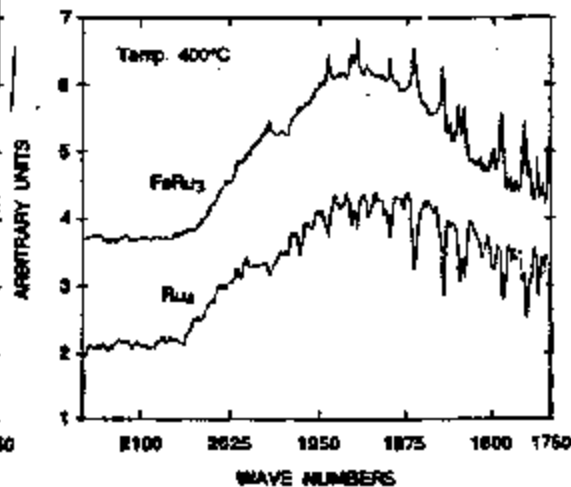
RA-2678-42



RA-2678-40



RA-2678-41



RA-2678-44

Figure 4: Comparison of Ru₄ and FeRu₃ clusters on MgO under CH₄.

REFERENCES

1. R. Pitchai and K. Klier, *Catal. Rev.-Sci. Eng.*, 28(1), 13-88 (1986).
2. H.L. Mitchell, III; R.H. Waghorne; U.S. Patent No. 4239658 (1980).
3. C.A. Jones, J.J. Leonard; J.A. Sofranko; U.S. Patent 4,554,395 (1985).
4. A. Frennet, *Catal. Rev.-Sci. Eng.*, 10(1), 37(1974).
5. M.E. Dry and J.C. Hoogendoorn, *Catal. Rev.*, 23, 265 (1981).
6. D.L. King, J.A. Cusumano, and R.L. Garten, *Catal. Rev.*, 23, 203 (1981).
7. H.C. Foley, S.J. D-Cani, K.D. T Au, K.J. Chao, J.H. Onuferko, C. Dybowski, and B.C. Gates, *J. Am. Chem. Soc.*, 105, 3074 (1983).
8. J.P. Candlin and H. Thomas, "Supported Organometallic Catalysis", in *Homogeneous Catalysis II*, D. Forster and J.F. Roth, eds., *Adv. Chem. Series*, 132, 212-239 (1974).
9. Y.I. Yermakov, B.N. Kuznetsov, and V.A. Zakharou, "Catalysis by Supported Complexes," Vol.8, *Studies in Surface Science and Catalysis*, Elsevier, Amsterdam, (1981).
10. A.A. Bhattacharyya, C.L. Nagel, and S.G. Shore, *Organometallics*, 2, 1187 (1983).
11. G.L. Geoffroy and W.L. Gladfelter, *J. Am. Chem. Soc.*, 99, 7565 (1977).
12. D.R. Stull, E.F. Westrum Jr., and G.C. Sinke, *The Chemical Thermodynamic of Organic Compounds*, Wiley, New York, (1969).
13. D.L. King, J.A. Cusumano, and R.L. Garten, *Catal. Rev.*, 23, 203 (1981).
14. H.C. Foley, S.J. D-Cani, K.D. T Au, K.J. Chao, J.H. Onuferko, C. Dybowski, and B.C. Gates, *J. Am. Chem. Soc.*, 105, 3074 (1983).
15. J.J. Venter and M.A. Vannice, *Applied Spectroscopy*, 42, 1096 (1988).